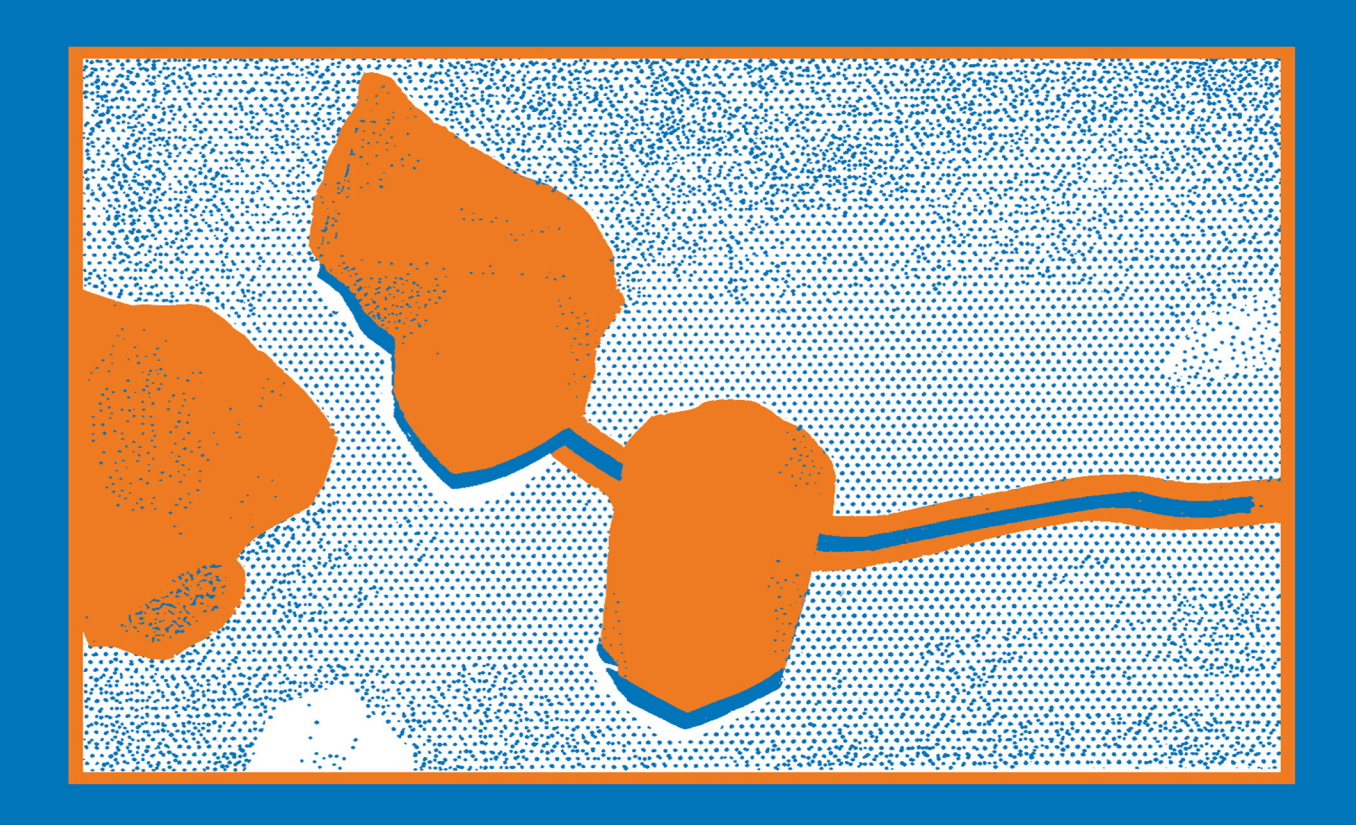
## Fracture of Brittle, Disordered Materials

**Concrete, Rock and Ceramics** 

Edited by

G. BAKER and B.L. KARIHALOO





Fracture of Brittle, Disordered Materials

CONCRETE, ROCK AND CERAMICS

# Fracture of Brittle, Disordered Materials

CONCRETE, ROCK AND CERAMICS

Proceedings of The International Union of Theoretical and Applied Mechanics (IUTAM) Symposium on Fracture of Brittle, Disordered Materials: Concrete, Rock and Ceramics, 20–24 September 1993, The University of Queensland, Brisbane, Australia

Edited by

G. BAKER

Department of Civil Engineering, The University of Queensland, Brisbane, Australia

and

**B.L. KARIHALOO** 

Department of Civil and Mining Engineering, The University of Sydney, Sydney, Australia



By Taylor & Francis, 2 Park Square, Milton Park, Abingdon, Oxon, OX14 4RN 270 Madison Ave, New York NY 10016

First edition 1995

Transferred to Digital Printing 2006

© 1995 Taylor & Francis

ISBN 0419190503

Apart from any fair dealing for the purposes of research or private study, or criticism or review, as permitted under the UK Copyright Designs and Patents Act, 1988, this publication may not be reproduced, stored, or transmitted, in any form or by any means, without the prior permission in writing of the publishers, or in the case of reprographic reproduction only in accordance with the terms of the licences issued by the Copyright Licensing Agency in the UK, or in accordance with the terms of licences issued by the appropriate Reproduction Rights Organization outside the UK. Enquiries concerning reproduction outside the terms stated here should be sent to the publishers at the London address printed on this page.

The publisher makes no representation, express or implied, with regard to the accuracy of the information contained in this book and cannot accept any legal responsibility or liability for any errors or omissions that may be made.

A catalogue record for this book is available from the British Library

#### **Publisher's Note**

This book has been produced from camera ready copy provided by the individual contributors.

The publisher has gone to great lengths to ensure the quality of this reprint but points out that some imperfections in the original may be apparent

#### **Contents**

	eface ientific Committee	i) X
KJ	EYNOTE ADDRESS	1
1	The scaling laws and renormalization group in the mechanics and micromechanics of fracture G.I. BARENBLATT	3
P.A	ART ONE FRACTURE MECHANICS OF CONCRETE	19
2	Multifractal nature of material microstructure and size effects on nominal tensile strength A. CARPINTERI, B. CHIAIA and G. FERRO	21
3	Tension softening diagrams and longitudinally reinforced beams B.L. KARIHALOO	35
4	The extended cohesive crack J. PLANAS, M. ELICES and G.V. GUINEA	51
5	On the cohesive crack model in mixed-mode conditions S. VALENTE	66
	ART TWO FRACTURE OF BRITTLE MATRIX OMPOSITES	81
6	Fracture mechanism of fiber reinforced quasi brittle matrix composites S.P. SHAH and Z. LI	83
7	Fracture and flexible behaviour in strain-hardening cementitious composites V.C. LI, M. MAALEJ and Y-M. LIM	101
8	Strength and toughness analysis of fibre reinforced brittle matrix composites A.A. RUBINSTEIN	116
9	Micromechanical parameters, fracture processes and application of fiber reinforced concrete H. STANG	131

PA	ART THREE FRACTURE MECHANICS OF ROCK	149
10	Micromechanics of non-linear macroscopic deformation and fracture of rocks under differential compression L.R. MYER, J.M. KEMENY, N.G.W. COOK, Z. LIU and K.T. NIHEI	151
11	Process-zone effect on the failure of rock-like materials J.F. LABUZ and L. BIOLZI	168
12	Anisotropic crack damage development in rock under cyclic triaxial loading: an acoustic emission and elastic wave velocity study C.E. STUART, P.G. MEREDITH, S.A.F. MURRELL and J.G. van MUNSTER	181
PA	ART FOUR FRACTURE MECHANICS OF CERAMICS	195
13	On the theoretical toughness and strength of ceramic composites B. BUDIANSKY	197
14	Crack growth in a sintered Al <sub>2</sub> O <sub>3</sub> /ZrO <sub>2</sub> composite subjected to monotonic and cyclic loading K. DUAN, Y-W. MAI and B. COTTERELL	212
15	Deformation and fracture in the frontal process zone and the crack-face contact region of a polycrystalline graphite M. SAKAI and H. KURITA	227
PA	PART FIVE CONTINUUM MODELS	
16	Continuum methods for localised failure R. de BORST, J. PAMIN, J.C.J. SCHELLEKENS and L.J. SLUYS	249
17	Compressive and shear failure modes in brittle materials Z. MRÓZ and M. KOWALCZYK	264
18	A continuum theory for random packings of elastic spheres HB. MÜHLHAUS and F. OKA	285
PA	ART SIX DISCRETE CRACK MODELS	299
19	Topology-controlled modeling of linear and nonlinear 3D crack propagation in geo-materials  B. I. CARTER, A.R. INCRAFERA and T.N. BITTENCOLIRT	301

	Contents vii
<ul> <li>Topological considerations for 3D computational fractumechanics</li> <li>C.A. GRUMMIT and G. BAKER</li> </ul>	are 319
<ul><li>Fracture analysis of concrete based on the discrete crace by the boundary element method</li><li>M. OHTSU and A.H. CHAHROUR</li></ul>	ek model 335
22 Fracture process zone associated with ceramic fracture experimental-numerical analysis C.T. YU and A.S. KOBAYASHI	- an 348
PART SEVEN MICROMECHANICS AND MICROMECHANICAL MODELS	359
23 On the micromechanics and fracture of ceramics V. TVERGAARD	361
<ul><li>On wave propagation in two-phase materials with interdefects</li><li>D. GROSS and Ch. ZHANG</li></ul>	<b>face</b> 376
<ul><li>Thermomechanics and micromechanics-based continuu for localization phenomena H. HORII and Y. OKUI</li></ul>	m theory 391
26 Micromechanical analysis and experimental verification boundary rotation effects in uniaxial tension tests on con J.G.M. van MIER and A. VERVUURT	
PART EIGHT DAMAGE, LOCALIZATION AN EFFECT	ID SIZE 421
<ul> <li>Continuum damage due to interacting propagating mic new nonlocal model and localization analysis</li> <li>P. BAŽANT and M. JIRÁSEK</li> </ul>	rocracks: 423
28 Thermodynamics of damage evolution in discretized sys D. KRAJCINOVIC and V. LUBARDA	stems 438
29 Recent research on the cohesive zone description of an softening material E. SMITH	elastic 450
30 Analysis of localized failure in elastoplastic solids H. YOSHIKAWA and K. WILLAM	464

#### viii Contents

	ART NINE APPLICATIONS OF FRACTURE ECHANICS	479
31	Offshore concrete platforms in Norway: materials and static analyses M. MODÉER	481
32	Application of fracture mechanics parameters to the design and lifetime prediction of ceramic components  A. BRÜCKNER-FOIT, T. FETT, A. HEGER and D. MUNZ	495
33	Numerical simulations of crack bifurcation in the chip forming cutting process in rock W.G.M. van KESTEREN	505
34	Anchorage and bond properties in concrete T. OLOFSSON, K. NOGHABAI, U. OHLSSON and L. ELFGREN	525
PA	ART TEN POSTER PRESENTATIONS	545
35	Boundary element analysis of transformation toughening test specimens J.H. ANDREASEN	547
36	Continuum models for simulation of excavation in regular jointed rock structures C. DAI, H. MÜHLHAUS, J. MEEK and M. DUNCAN FAMA	552
37	Short crack fatigue in ZTC M.H. JØRGENSEN	559
38	Simple application of fictitious crack model in reinforced concrete beams  J.P. ULFKJÆR, O. HEDEDAL, I. KROON and R. BRINCKER	564
39	A micromechanics-based continuum theory for rock masses containing fracturing joints H. YOSHIDA and H. HORII	569
Author index Subject index		575 577

### 17 COMPRESSIVE AND SHEAR FAILURE MODES IN BRITTLE MATERIALS

Z. MRÓZ and M. KOWALCZYK Institute of Fundamental Technological Research, Warsaw, Poland

#### Abstract

In brittle materials failure modes develop consecutively producing very frequently periodic sequence of failure events. Under compression, the cracking mode develops first, thus producing a set of oriented cracks inducing stress redistribution and anisotropic response. The crushing and post-buckling modes are associated with subsequent failure of cracked portions due to localized shearing or loss of stability.

The progression of particular modes is discussed by assuming existence of discontinuity interfaces between modes with proper evolution rules. An incremental problem associated with moving interface is formulated. The evolution rate of the interface follows from the energy condition of propagation of a set of cracks (cracking interface).

Several examples are treated in detail. Cracking and crushing around a circular hole is considered first. Next, this analysis is applied to study a rigid punch indentation into a plate. The oscillatory character of force variation is exhibited theoretically and confronted with experimental observations.

Keywords: Cracking, Crushing, Buckling, Indentation, Limit Load, Post-critical State.

#### 1 Introduction

The present paper is devoted to the analysis of progressive failure modes in brittle materials, such as rock, ice, concrete, or ceramics. The constitutive models for such materials are usually concerned with description of deformation response in stable regime before the onset of localization and loss of stability after reaching the maximal stress, cf. Jaeger and Cook (1976), Derski et al (1989). The post-critical stress-strain response was measured in some compression tests with the control set on circumferential strain. However, there is no general methodology developed so far in treatment of boundary-value problems associated with both stable and post-critical regimes. In many technical problems such as rock crushing, cutting of

drilling, ice-plate interaction with off-shore platforms, etc., all progressive modes should be accounted for in order to predict realistically the interaction pressures and the sequence of failure modes. The present paper is devoted to these problems and the necessary simplifying assumptions are introduced in order to provide analytical solutions. In particular, we shall distinguish such modes as cracking, crushing, shearing, and buckling. These modes are assumed to propagate within the loaded material with proper interaction along interfaces. It will be shown that the evolution of progressive failure modes induces periodicity of failure events with the associated oscillatory character of a load-displacement curve.

In Section 2, the material model assumptions are presented and the evolution problem of distinct damage zones will be formulated in an incremental form. In Section 3, the analysis of progression of cracked and crushed zones in the axisymmetric case is discussed. In Section 3, the punch penetration problem is analysed in the case of plane strain and plane stress, with the respective load-displacement curve exhibiting oscillatory character associated with initiation and termination of consecutive failure events. The reference to experimental observation will be provided.

#### 2 Material Model and Problem Formulation

Consider a problem illustrated in Fig. 1. The plane structure  $\mathcal{B}$  of a brittle material is rigidly supported on the boundary  $S_u$  and loaded by a compressive traction  $T^0$  on the boundary portion  $S_T$ . It is assumed that compressive loading induces progressive cracking of the material. The cracks are assumed to follow the trajectories of the major compressive stresses (or be perpendicular to the major tensile strain trajectories), Fig. 1. For increasing load, the cracked domain increases with its interface  $S_d$  moving into the undamaged domain. It is assumed that the stiffness moduli at the interface vary discontinuously. In fact, the cracked domain is characterized by an orthotropic stiffness matrix with vanishing stiffness in the direction normal to the crack trajectories. For further increase of load, the primary crack pattern is changed by generation of cracks inducing consecutive fragmentation through shearing of strips between primary cracks. Alternatively, buckling of strips may occur within the structure plane or in the transverse direction. This second mode of failure will be called the crushing mode and the interface S2 separates the crushing and cracking domains, Fig. 1b. The ultimate failure will correspond to flow of crushed material to the free surface within the plane or to lateral post-buckling with localised bending for a thin plate.

The present assumptions constitute a simplified model of cracking and crushing zone propagation as in actuality there is a gradual transition from one to the other mode. Instead of considering propagation condition for each crack, we assume the moving interface to represent all cracks growth. The proper energy condition can then be formulated, similar to the Griffith condition for a single crack.

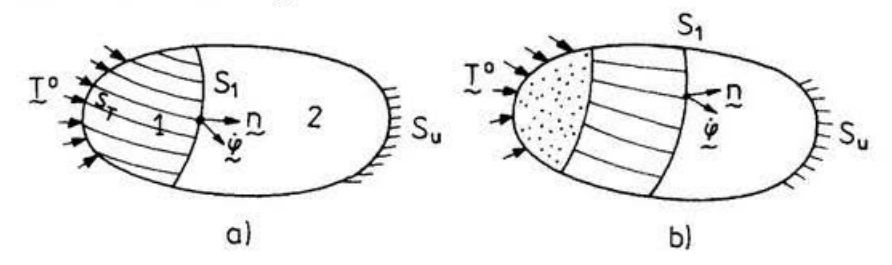


Figure 1: a) Propagation of cracked zone b) Propagation of crushed and cracked zones

Denote by u,  $\varepsilon$ , and  $\sigma$  the displacement, strain and stress states. The states within the intact domain be denoted by subscript 2 and within the damage zone by subscript 1. On the interface  $S_1$ , the tractions and displacements are continuous, thus,

$$[u] = 0 [T] = [\sigma n] = 0 on S_1 (1)$$

where  $[u] = u_2 - u_1$  denotes the discontinuity of u and similar notation applies to other fields. However, the displacement gradients, strain and stress fields are discontinuous, so that

$$u_{i,j} = a_i n_j$$
  $\left[\varepsilon_{ij}\right] = \frac{1}{2}(a_i n_j + a_j n_i)$  on  $S_1$  (2)

where a denotes the discontinuity vector and n is the unit normal on  $S_1$  directed into the undamaged domain. Assume the damaged and undamaged materials to satisfy the linear relations

$$\sigma_1 = C_1(\varepsilon_1 - \varepsilon_1^i)$$
  $\sigma_2 = C_2(\varepsilon_2 - \varepsilon_2^i)$  (3)

where  $C_1$  and  $C_2$  are the elasticity matrices and  $\boldsymbol{\varepsilon}_1^i$ ,  $\boldsymbol{\varepsilon}_2^i$  are the inelastic or initial strains. In view of (1) and (2), the following equation is obtained to specify the discontinuity vector  $\boldsymbol{a}$ 

$$A_2 a = b \quad \text{or} \quad A_{(2)jk} a_k = b_j \tag{4}$$

where

$$A_2 = n C_2 n \qquad b = -n [C] \epsilon_1 - n C_1 \epsilon_1^i + n_2 C_2 \epsilon_2^i \qquad (5)$$

Here  $A_2$  denotes the acoustic tensor and b is the interface "force vector".

The propagation of interface will now be considered as an evolution process specified by the transformation velocity  $\dot{\varphi}(x,t)$ . When the interface  $S_1$  moves, the first equation (1) provides

$$[\dot{u}_i] = \left[\frac{\partial u_i}{\partial t}\right] + u_{i,j}\dot{\varphi}_j = \left[\frac{\partial u_i}{\partial t}\right] + a_i\dot{\varphi}_n = 0 \tag{6}$$

so that

$$\left[\dot{u}_i\right] = \left[\frac{\partial u_i}{\partial t}\right] = -a_i \dot{\varphi}_n$$
 (7)

where  $\dot{\varphi}_n = \dot{\varphi}_i n_i$  denotes the normal propagation velocity component,  $\dot{u}_i$  denotes the total time derivative and  $\partial u_i/\partial t$  is the local derivative. The second equation (1) now provides the traction continuity condition

$$\left[\dot{T}_{i}\right] = \left[\frac{\partial \sigma_{ij}}{\partial t}\right] n_{j} + \left[\frac{\partial \sigma_{ij}}{\partial x_{k}}\right] n_{j} \dot{\varphi}_{k} = 0 \tag{8}$$

As the time derivative of the unit vector n is

$$\dot{n}_{j} = (n_{j}n_{l} - \delta_{jl})n_{k}\dot{\varphi}_{k,l} \tag{9}$$

we obtain the local stress rate discontinuity condition

$$\left[\dot{\bar{\sigma}}_{ij}\right]n_j = \left[\frac{\partial \sigma_{ij}}{\partial t}\right]n_j = \left[\sigma_{il}\right]n_k \dot{\varphi}_{k,l} - \left[\frac{\partial \sigma_{ij}}{\partial x_k}\right]n_j \dot{\varphi}_k \tag{10}$$

Equations (7) and (10) provide the boundary conditions for the rate problem associated with propagation of interface. Denoting by  $\dot{\sigma}_1$ ,  $\dot{\epsilon}_1$ ,  $\dot{u}_1$ , and by  $\dot{\sigma}_2$ ,  $\dot{\epsilon}_2$ ,  $\dot{u}_2$ , the local rates of state fields in two body portions, we can write the equilibrium and boundary conditions for those rates, namely

$$\dot{\bar{\sigma}}_{(1)ij,j} = 0 \qquad \dot{\bar{\sigma}}_1 = C_1 \dot{\bar{\epsilon}}_1 
\dot{\bar{\sigma}}_{(1)ij} n_j = 0 \text{ on } S_T \qquad \dot{\bar{u}}_{(1)i} = 0 \text{ on } S_u$$
(11)

and similar equations within the undamaged domain. The interface discontinuity conditions (7) and (10) then provide supplementary equations generating non-vanishing solutions. Let us note that we have now a non-typical boundary value problem when discontinuities in both displacement and traction rates are specified on the interface  $S_u$ .

The stability conditions associated with moving damage interface were discussed in detail by Dems and Mróz (1985) where the limit state criteria were derived. The relevant stability criteria for a system of cracks in a brittle solids were derived by Bažant and Ohtsubo (1977).

The generalized forces associated with interface propagation can be derived by considering the variation of potential or complementary energies of the body. The potential energy

$$\Pi(\mathbf{u}, S_1) = \int U(\boldsymbol{\varepsilon})dV - \int \mathbf{T}^0 \cdot \mathbf{u}dS_T$$
 (12)

is now a function of both displacement field and interface position. The variation of  $\Pi$  equals

$$\dot{\Pi} = \int \frac{\partial U}{\partial \varepsilon} \cdot \dot{\varepsilon} dV + \int [U] \dot{\varphi}_n dS_1 \tag{13}$$

where  $U(\varepsilon)$  is the specific strain energy. However, in view of the virtual work principle and (6), there is

$$\int \boldsymbol{\sigma} \cdot \dot{\boldsymbol{\epsilon}} dV = \int \boldsymbol{T} \cdot \left[ \dot{\boldsymbol{u}} \right] dS_1 = - \int \boldsymbol{T} \cdot \boldsymbol{\alpha} \dot{\varphi}_n dS_1 \qquad (14)$$

and (14) can be expressed as follows

$$\dot{\Pi}(\boldsymbol{u}, S_1) = \int ([U] - \boldsymbol{T} \cdot \boldsymbol{a}) \dot{\varphi}_n dS_1 = \int H \dot{\varphi}_n dS_1$$
 (15)

where

$$H = [U] - \mathbf{T} \cdot \mathbf{a} \tag{16}$$

is the generalized force associated with the interface propagation.

An alternative expression for the force H can be obtained by decomposing stress and strain at the interface into "exterior" and "interior" or hidden portions  $\sigma^b$ ,  $\sigma^h$  and  $\varepsilon^b$ ,  $\varepsilon^h$ . In a local orthogonal system  $n, \alpha, \beta$ , the external stress  $\sigma^b$  corresponds to the interface traction and is represented by the components  $\sigma_{nn}$ ,  $\sigma_{n\alpha}$ ,  $\sigma_{n\beta}$ . Similarly, the external strain  $\varepsilon^b$  is represented by the components  $\varepsilon_{nn}$ ,  $\varepsilon_{n\alpha}$ ,  $\varepsilon_{n\beta}$ . Since at the interface there is  $[\sigma^b] = 0$  and  $[\varepsilon^h] = 0$ , we have

$$[\boldsymbol{\sigma} \cdot \boldsymbol{\varepsilon}] = \left[\boldsymbol{\sigma}_b \cdot \boldsymbol{\varepsilon}^b + \boldsymbol{\sigma}_h \cdot \boldsymbol{\varepsilon}^h\right] = \boldsymbol{\sigma}^b \cdot \left[\boldsymbol{\varepsilon}^b\right] + \left[\boldsymbol{\sigma}^h\right] \cdot \boldsymbol{\varepsilon}^h \tag{17}$$

and the generalized force is

$$H = [U] - \mathbf{T} \cdot \mathbf{a} = \frac{1}{2} \left( \boldsymbol{\sigma}^b \cdot \left[ \boldsymbol{\varepsilon}^b \right] + \left[ \boldsymbol{\sigma}^h \right] \cdot \boldsymbol{\varepsilon}^h - \boldsymbol{\sigma}^b \cdot \left[ \boldsymbol{\varepsilon}^b \right] \right) = \frac{1}{2} \left( \left[ \boldsymbol{\sigma}^h \right] \cdot \boldsymbol{\varepsilon}^h - \boldsymbol{\sigma}^b \cdot \left[ \boldsymbol{\varepsilon}^b \right] \right)$$

$$(18)$$

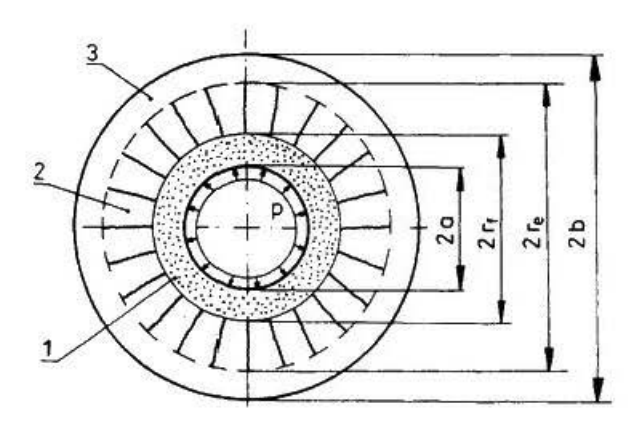


Figure 2: Axisymmetric cylinder with different stress stage zones: 1) crushed 2) cracked 3) elastic

This expression will be used in analysing the damage interface propagation.

#### 3 Axisymmetric Cracking and Crushing Modes

Let us first consider an axisymmetric problem of a cylinder acted on by internal pressure and in the limit case of a hole in an infinite continuum. For the plane strain case, the material is assumed to be in elastic, cracking or crushing state developed in the course of progressive deformation. Figure 2 presents the respective states within the cylinder. The detailed analysis was presented by Kowalczyk and Mróz (1988) following previous studies by Ladanyi (1967) and Hellan (1984).

Assume the macrocracks to develop along radial directions and the cracked material to be regarded as an orthotropic material of vanishing stiffness moduli in circumferential direction. The total strain components  $\varepsilon_{\tau}$  and  $\varepsilon_{t}$  in radial and circumferential directions are decomposed in the cracked zone as follows

$$\varepsilon_r = \varepsilon_r^e + \varepsilon_r^f$$
  $\varepsilon_t = \varepsilon_t^e + \varepsilon_t^f$  (19)

where  $\varepsilon_r^c, \varepsilon_t^c$  are the elastic strains and  $\varepsilon_r^f, \varepsilon_t^f$  are the fracture strains. In the crushed zone, the material is assumed to behave like an isotropic granular medium in the limit equilibrium state specified be the Coulomb yield condition. We have therefore

$$\varepsilon_r = \varepsilon_r^e + \varepsilon_r^p \qquad \varepsilon_t = \varepsilon_t^c + \varepsilon_t^p$$
 (20)

where  $\varepsilon_r^p, \varepsilon_t^p$  are the plastic strains.

The equilibrium equations are

$$\frac{\partial \sigma_r}{\partial r} + \frac{\sigma_r - \sigma_t}{r} = 0 \tag{21}$$

and the strain displacement relations take the form

$$\varepsilon_r = \frac{\partial u}{\partial r}$$
  $\varepsilon_t = \frac{u}{r}$  (22)

In the elastic zone, the Hookes law for an isotropic material applies, thus

$$\varepsilon_r^{\epsilon} = \frac{1+\nu}{E} [(1-\nu)\sigma_r - \nu\sigma_t]$$
  $\varepsilon_t^{\epsilon} = \frac{1+\nu}{E} [(1-\nu)\sigma_t - \nu\sigma_r]$  (23)

In the cracked zone there is

$$\varepsilon_r^f = 0$$
  $\sigma_t = 0$   $\varepsilon_t^f > 0$  (24)

Assume the cracked zone to contain many cracks propagating from the internal boundary r=a to the interface boundary  $r=r_e$ . Using the Griffith condition of crack propagation, the potential energy release calculated at the progressing interface  $r=r_e$  is assumed to be equal to fracture toughness of n cracks, so that

$$H2\pi r_{e} = nK_{Ic}^{2} \frac{(1-\nu^{2})}{E}$$
 (25)

or using (18), we have

$$\pi r_e \left[ \sigma_t^2(r_e) \right] = n K_{Ie}^2 \qquad (26)$$

The crushed zone follows the cracked zone for increasing internal pressure and the material is assumed to satisfy the Coulomb yield condition

$$F_1 = \sigma_t - \sigma_r + (\sigma_t + \sigma_r)\sin\varphi - 2C\cos\varphi = 0 \qquad F_3 = \sigma_r - S_t = 0$$

$$F_2 = \sigma_r - \sigma_t + (\sigma_t + \sigma_r)\sin\varphi - 2C\cos\varphi = 0 \qquad F_3 = \sigma_t - S_t = 0$$

$$(27)$$

where the initial cohesion equals  $C_0$  and in passing to a crushed state it drops to the residual value  $C_r = 0$ . Similarly, the initial tensile strength  $S_t$  drops to zero when cracks develop. The friction angle  $\varphi$  is assumed constant during the process. Here  $F_1 = 0$ ,  $F_2 = 0$  represent the shear mode and  $F_3 = 0$ ,  $F_4 = 0$  correspond to the tensile mode of flow. The flow rule specifies the plastic strain rates, namely

$$\dot{\varepsilon}_{\tau}^{p} = \dot{\lambda} \frac{\partial g_{i}}{\partial \sigma_{\tau}} \qquad \dot{\varepsilon}_{t}^{p} = \dot{\lambda} \frac{\partial g_{i}}{\partial \sigma_{t}} \tag{28}$$

where  $\dot{\lambda}$  and  $g_i(i=1,2,3,4)$  specify the plastic potentials

$$g_1 = \sigma_t - \sigma_r + (\sigma_t + \sigma_r) \sin \psi - 2C_g \cos \psi = 0$$

$$g_2 = \sigma_r - \sigma_t + (\sigma_t + \sigma_r) \sin \psi - 2C_g \cos \psi = 0$$
(29)

where  $\psi$  is the dilatancy angle. The potentials  $g_3$  and  $g_4$  are assumed to be identical to  $F_3 = 0$ ,  $F_4 = 0$ .

#### 3.1 Solutions for specific zones

At the initial stage, the elastic zone occurs within the whole cylinder. The stress and strain distribution are governed by Lame equations, so that

$$u = \frac{1+\nu}{E} \frac{p_e r_e^2}{b^2 - r_e^2} \left[ (1-2\nu)r + \frac{b^2}{r} \right]$$

$$\sigma_r = \frac{p_e r_e^2}{b^2 - r_e^2} \left( 1 - \frac{b^2}{r^2} \right) \qquad \sigma_t = \frac{p_e r_e^2}{b^2 - r_e^2} \left( 1 + \frac{b^2}{r^2} \right)$$
(30)

where  $r_{\epsilon} = a, p_{\epsilon} = p$ . The critical pressure initiating cracking now is

$$p_c = S_t \frac{b^2 - a^2}{b^2 + a^2} \tag{31}$$

The second phase,  $r_{\rm c} > a, r_f = a$  corresponds to existence of two zones: elastic and cracked. In the elastic zone, the Lame solution applies with internal zone radius specifying the interface between cracked and elastic zones. The pressure acting on the interface is obtained from the solution for two zones and the crack propagation condition must be satisfied at  $r = r_{\rm c}$ .

In the cracked zone we have

$$u = \frac{1 - \nu^2}{E} A_1 \ln r + A_2$$

$$\sigma_r = \frac{A_1}{r} \qquad \sigma_t = 0$$
(32)

where the integration constants  $A_1$  and  $A_2$  follow from the radial stress and displacement continuity at  $r=r_\epsilon$ :  $[\sigma_r(r_\epsilon)]=[u_r(r_\epsilon)]=0$ . Using the condition  $\sigma_r(r_f)=p$  and the cracking condition (26) at  $r=r_\epsilon$ , the relation between the radius  $r_\epsilon$  of cracked zone and the pressure  $p_\epsilon$  at  $r=r_\epsilon$  is

$$p_{\epsilon} = K_I \sqrt{\frac{n}{\pi r_{\epsilon}}} \frac{b^2 - r^2}{b^2 + r^2} \tag{33}$$

Since at the onset of crack propagation there is  $r_e = a, p_e = p_c$ , hence in view of (31) and (33), there is

$$S_t = K_I \sqrt{\frac{n}{\pi a}} \tag{34}$$

The internal pressure within the tube is now explicitly related to the size of cracked zone, namely

$$p = S_{\ell} \sqrt{\frac{r_e}{a}} \frac{b^2 - r_e^2}{b^2 + r_e^2}$$
(35)

The relation  $p(r_e)$  exhibits limit point at the critical crack length  $r_{ec} = b(\sqrt{17} - 4)^{1/2}$  for which  $p_c = 0.4625 S_t \sqrt{b/a}$ . The loading process is unstable for  $r_e > r_{ec}$ .

As in the cracked zone there is a uniaxial stress state,  $\sigma_r \neq 0$ ,  $\sigma_t = 0$ , the crushing starts when the pressure p exceeds the compressive strength  $S_c$ . Thus, for  $p > S_c$ , the crushed zone propagates from the internal cylinder boundary. The equilibrium equations (21) and the yield condition (27) provide the static field

$$\sigma_{\tau} = A_3 r^{\alpha_1 - 1}$$
  $\sigma_t = \alpha_1 A_3 r^{\alpha_1 - 1}$  (36)

where A3 is the integration constant and

$$\alpha_1 = \frac{1 - \sin \varphi}{1 + \sin \varphi} \tag{37}$$

Substituting (36) into the Hookes law, the elastic strains are calculated, namely

$$\varepsilon_r^{\epsilon} = \frac{1+\nu}{E} (1-\nu-\nu\alpha_1) A_3 r^{\alpha_1-1}$$

$$\varepsilon_t^{\epsilon} = \frac{1+\nu}{E} [(1-\nu)\alpha_1 - \nu] A_3 r^{\alpha_1-1}$$
(38)

Next, using the flow rule (28) and integrating plastic strain rates, we have

$$\varepsilon_r^p = -\lambda(1 - \sin \psi)$$
  $\varepsilon_t^p = \lambda(1 + \sin \psi)$   $\lambda > 0$  (39)

so that

$$\varepsilon_{\tau}^{p} = -\alpha_{2}\varepsilon_{t}^{p} \qquad \alpha_{2} = \frac{1 - \sin\psi}{1 + \sin\psi} \tag{40}$$

and the plastic strain distribution is obtained from the compatibility condition

$$\varepsilon_{\tau}^{\epsilon} + \varepsilon_{\tau}^{p} = \frac{d}{dt} \left[ r(\varepsilon_{t}^{\epsilon} + \varepsilon_{t}^{p}) \right] \tag{41}$$

Finally, we obtain

$$\varepsilon_{t}^{p} = \frac{1 - \nu^{2}}{E} \frac{1 - \alpha_{1}^{2}}{\alpha_{1} + \alpha_{2}} A_{3} r^{\alpha_{1} - 1} + A_{4} r^{-(\alpha_{2} + 1)}$$

$$u = \frac{1 + \nu}{E} \left[ (1 - \nu) \frac{1 + \alpha_{1} + \alpha_{2}}{\alpha_{1} + \alpha_{2}} - \nu \right] A_{3} r_{1}^{\alpha} + A_{4} r^{-\alpha_{2}}$$
(42)

where the integration constants are determined from the continuity conditions for tractions and displacements on the interface between crushed and cracked zones

$$[\sigma_{\tau}(r_f)] = [u_{\tau}(r_f)] = 0$$
 (43)

and  $\sigma_r(r_{c_1}) = p_{c_1}$ . For the critical value of  $r_f$  the pressure reaches its maximum and the unstable phase begins. However, for an infinite value of b, that is for the case of hole in an infinite body, the deformation process is stable and continuing progression of crushed and cracked zones occurs. The pressure acting at  $r = r_f$  now is

$$p_f = S_t \sqrt{\frac{r_e}{r_{fe}}} \frac{b^2 - r_e^2}{b^2 + r_e^2} \tag{44}$$

The detailed analysis of unloading zones for a cylinder was presented by Kowalczyk and Mróz (1988). To illustrate the solution we present the zone evolution for

$$\frac{S_t}{E} = 0.001$$
  $\frac{C_0}{E} = 0.0012$   $\nu = 0.3$   $\varphi = \psi = 20^{\circ}$  (45)

Figure 3 presents the diagram of pressure dependence on the size of the cracked zone and Fig. 4 provides the pressure displacement diagrams. In the next example, the solution for  $b/a = \infty$  will be applied to study punch penetration.

#### 4 Punch penetration into a brittle material

The axisymmetric solution of the preceding section will now be used to construct a simplified solution of punch indentation in plane strain and plane stress cases. When a rigid punch is penetrated into an elastic semiplane, the stress concentration zones at punch edges induce localized cracking and crushing beneath the punch, cf. experimental data in papers by Pang et al (1989), (1990), Swain and Lawn (1976), Tokar (1990), Wagner and Schümann (1971), Wijk (1989), Lindqvist and Lai (1983). It is assumed that a crushed zone of radius  $r_f$  is formed with the hydrostatic stress state. This zone acts as a pressure loading on the remaining material thus inducing cracking and subsequent shearing or buckling of the cracked material blocks. It is assumed that the cracked zone is bounded by a circle of radius  $r_e$  and radial lines  $\tau = \pm \alpha_f$ , Fig.3. The cracks are assumed to

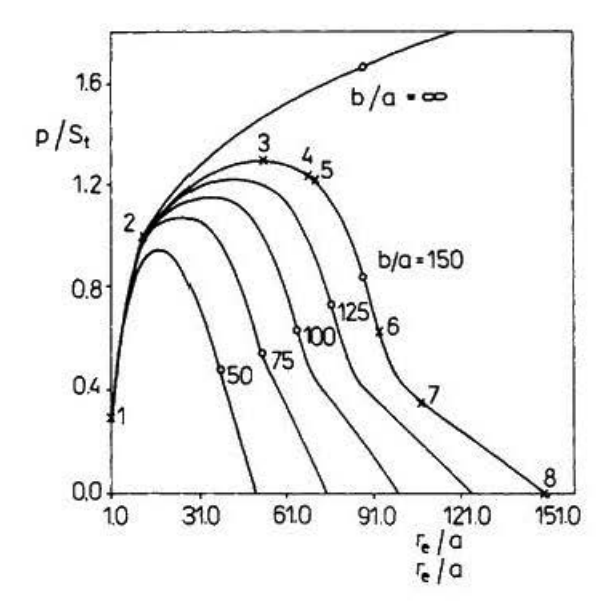


Figure 3: Pressure dependence on the size of cracked zone

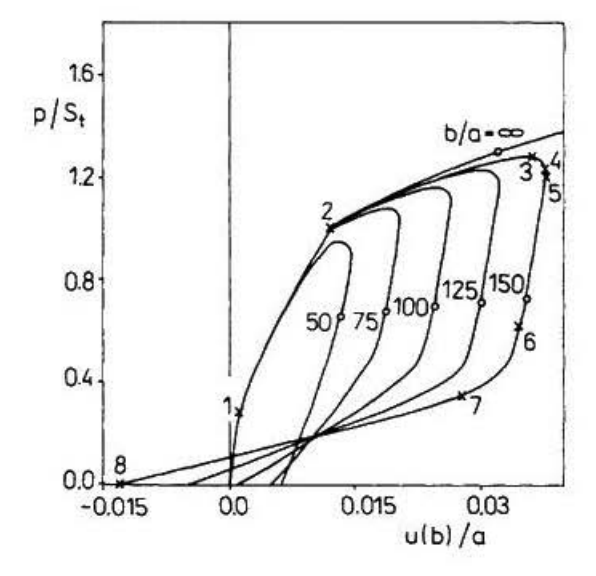


Figure 4: Pressure dependence on the internal surface displacement

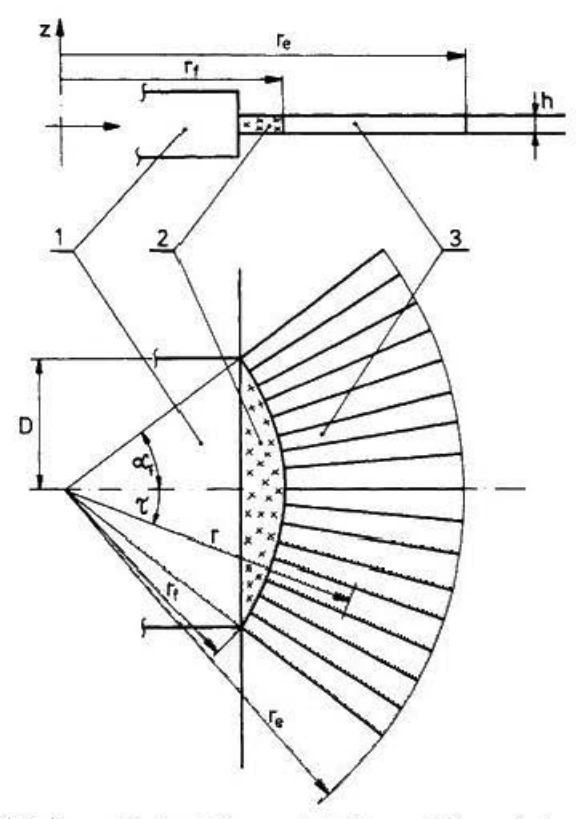


Figure 5: Simplified punch indentation model: 1) punch 2) crushed zone 3) cracked zone

propagate along radial directions, so the axisymmetric solution can be assumed to predict the radius  $r_e$  of the cracked zone. For simplicity, we neglect the progressive crushing and growth of the initial crushed zone of radius  $r_f$ . The subsequent failure mode within the plane develops in a form of localized shearing along velocity discontinuity lines, inducing motion of material toward the free surface. For an elastic-plastic material the stage of development of localized shear bands should be considered. However, we assume that the failure mechanism develops instantaneously similarly as in rigid-plastic materials. On the other hand, in-plane stress state, the cracked beams are assumed to buckle in the out-of-plane mode and subsequently they deform in a post-buckling stage until total failure of beams occurs due to bending fracture of end cross-sections.

The post-critical stage is analysed by assuming the beams to be rigid with end cross-sections connected to the foundation by nonlinear springs of specified

characteristics. These simplified assumptions are introduced in order to generate the analytical solution before more accurate incremental analysis will be provided.

#### 4.1 Progression of cracking zone

Assuming the crushed zone to be fixed and specified by the radius  $r_f = a$ , the axisymmetric solution will be applied setting  $b \to \infty$ . The cracking condition now is assumed in the form

$$\sigma_t(r_e) = S_t \left(\frac{r_f}{r_e}\right)^{\kappa} = S_t \left(\frac{a}{r_e}\right)^{\kappa} \tag{46}$$

where  $\kappa$  is a positive exponent. For  $\kappa=0$  we obtain the strength condition and for  $\kappa=\frac{1}{2}$  the energy condition. By selecting proper value of  $\kappa$ , one can account for the fact that now cracking develops within an annular segment of unspecified angle  $\alpha_f$  and of number of cracks. The constants  $A_1$  and  $A_2$  occurring in (32) are now obtained from displacement and radial stress continuity conditions, so that

$$A_{1} = -S_{t}r_{e} \left(\frac{r_{f}}{r_{e}}\right)^{\kappa}$$

$$A_{2} = \frac{1+\nu}{E}S_{t}r_{e} \left(\frac{r_{f}}{r_{e}}\right)^{\kappa} \left[1 + (1-\nu)\ln(r_{e})\right]$$
(47)

The pressure  $p_e$  is calculated from (46). Since  $p_f = -\sigma_r(r_f)$  the pressure in the crushed zone beneath the punch is

$$p_f = S_t \left(\frac{r_f}{r_s}\right)^{\kappa - 1} \tag{48}$$

For  $0 < \kappa < 1$ , the growth of the fracture zone requires monotonic growth of punch pressure. Hence for some value  $r = r_{ec}$ , a new failure mode is to develop within the fractured zone.

#### 4.2 Shear failure (plane strain case)

The second failure mode is assumed in a form of limit failure mechanism developed both in cracked zone and undamaged zones, typical for limit analysis, Fig.4. The shear planes  $A_0A_1$ ,  $A_0A_2$ ,  $A_1A_2$  and  $A_2A_3$  constitute kinematically admissible failure mechanism. However  $A_0A_1$ ,  $A_0A_2$ ,  $A_1A_2$  are passed through the cracked zone of reduced cohesion. On the other hand,  $A_2A_3$  passes through the undamaged material so the initial cohesion and angle of friction should be used in calculating the dissipation rate. The balance of rate work and internal dissipation now is, cf. Mróz and Drescher (1968)

$$2DpV_0 = 2Cl_2V_2\cos\varphi \tag{49}$$

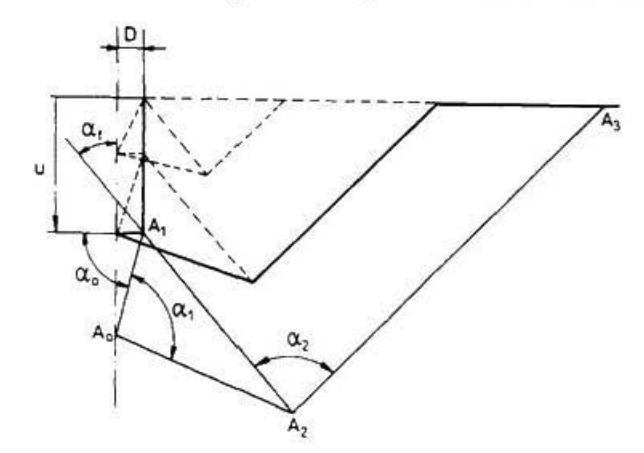


Figure 6: Kinematically admissible failure mechanism (third cycle in plane strain case)

where D is the punch half-width,  $l_2$  denotes the length of the discontinuity line  $A_2A_3$ ,  $V_0$  is the punch velocity and  $V_2$  is the velocity of block  $A_1A_2A_3$ . In writing (49) we neglect the residual cohesion on  $A_0A_2$   $A_2A_1$  and  $A_0A_1$  assuming it to be much smaller then  $C_0$ . Using hodograph and geometric relations, we obtain

$$p = C_0 \left( \frac{u_f}{D} + \frac{\sin \alpha_1 \cos \alpha_f}{\cos \alpha_0 \cos(\alpha_0 - \alpha_1 - \alpha_f)} \right)$$

$$\frac{\cos(\alpha_0 - \varphi) \cos(\alpha_0 - \alpha_1 - \alpha_f + 2\varphi) \cos \varphi}{\sin(\alpha_1 - 2\varphi) \sin(\alpha_2 - 2\varphi) \cos(\alpha_2 - \alpha_f)}$$
(50)

where the angles  $\alpha_0$ ,  $\alpha_1$ ,  $\alpha_2$  and the displacement  $u_f = u(r_f)$  are shown in Fig.4. The critical pressure is obtained by determining the minimum of  $p(\alpha_0, \alpha_1, \alpha_2)$  with respect to failure mode angles  $\alpha_0, \alpha_1, \alpha_2$ .

#### 4.3 Buckling failure (plane stress case)

In the case of plate thickness h small with respect to punch width 2D, the plane stress condition prevails and the cracked material can be regarded as a set of tapered beams supported at  $r=r_e$ . The out-of-plane buckling mode of beams is therefore considered. The post-buckling response induces localized cracking and softening at  $r=r_e$ , which involve decreasing load acting on the beam.

Denoting  $k = r_f/r_e$ , and introducing the plane stress elastic constants  $\nu_n = \nu/(1+\nu)$ ,  $E_n = E(1+2\nu)/(1+\nu)^2$ , we obtain the punch displacement and

pressure in the form

$$u_f = \frac{S_t r_f}{E_r \sqrt{k}} [(1 + \nu) - \ln(k)] \qquad p_f = \frac{S_t}{\sqrt{k}}$$
 (51)

Denote by  $b_{\epsilon}$  and  $b_f$  the widths of cracked beams at  $r = r_{\epsilon}$  and  $r = r_f$ , by  $F = p_f h b_f$  the force acting on beam of length  $l = r_{\epsilon} - r_f$ . Depending on geometric parameters the buckling mode can occur within the plane or out-of-plane. The corresponding critical taper ratios are denoted by  $k_t$  and  $k_z$ . The following relations specify  $k_t$  and  $k_z$  at buckling

$$\frac{b_{\epsilon}(k_{t})}{48l^{2}(k_{t})}\theta_{t}(k_{t})E_{n}h^{3} - p_{f}(k_{t})hb_{f} = 0$$

$$\frac{b_{\epsilon}(k_{z})}{48l^{2}(k_{z})}\theta_{z}(k_{z})E_{n}h^{3} - p_{f}(k_{z})hb_{f} = 0$$
(52)

where  $\theta_t$  and  $\theta_z$  denote the buckling coefficients provided by Życzkowski (1956) in the tabular form. It follows from (51) that the critical taper ratio  $k_c$  and buckling mode are determined by the condition  $k_c = \max(k_t, k_z)$ . The values of  $k_c$  and  $k_f$  are

$$b_e = \frac{b_f}{k} \qquad b_f = \frac{2}{n-1} \alpha_f r_f \qquad (53)$$

where n denotes the number of cracks and  $\alpha_f = \arccos(D/r_f)$  is the opening angle of the cracked zone.

The post-buckling analysis is carried out by assuming the buckled bar as rigid with the inelastic hinge support at  $r=r_{\epsilon}$ . The bending moment  $M_g$  at the hinge depends on the rotation angle  $\vartheta$  according to the relations

$$M_{g}(\vartheta) = \begin{cases} C_{\vartheta}\vartheta & \text{if } \vartheta \leq \vartheta_{0} \\ C_{\vartheta}\vartheta_{0} - C_{1}(\vartheta - \vartheta_{0}) & \text{if } \vartheta_{0} < \vartheta \leq \vartheta_{1} \\ 0 & \text{if } \vartheta_{1} < \vartheta \end{cases}$$

$$(54)$$

where  $\vartheta_0$  and  $\vartheta_1$  denote critical values of  $\vartheta$  indicating the onset and termination of the hinge failure process. Here  $C_0$  denotes the hinge stiffness in the elastic stage and  $C_1$  is the postcritical softening modulus. The value of  $C_0$  is obtained from the value of the critical buckling load,  $C_0 = F(k_c)l(k_c)$ . The value of  $\vartheta_0$  is obtained by assessing the rupture stress of material fibers in tension, so that

$$S_{t} = -6 \frac{F(k_{c})l(k_{c})\vartheta_{0}}{b_{c}h^{2}}$$
(55)

where compressive stress was neglected. The value of  $\vartheta_0$  evaluated for ice is of the order  $10^{-5}$ . Higher values can be obtained by accounting for the compressive stress, thus

$$S_t = -\frac{F(k_c)}{b_c h^2} \vartheta_0 [h \operatorname{ctg} \vartheta_0 + 6l(k_c)]$$
(56)

The value of  $\vartheta_1$  corresponds to  $M_g(\vartheta_1) = 0$ . The punch displacement and stress vary in the postcritical stage according to the relations

$$u_f = \frac{S_t r_f}{E_n \sqrt{k}} [(1+\nu) - \ln(k_c)] + l(k_c)(1-\cos\vartheta)$$

$$p_f = \frac{M_g(\vartheta)}{l(k_c)h b_f \sin\vartheta}$$
(57)

When  $\vartheta = \frac{1}{2}\pi$ , the consecutive loading cycle commences and the periodic sequence of cracking, buckling, post-buckling modes develops.

#### 4.4 Discussion of theoretical solutions

For numerical analysis, the following parameters were assumed

$$S_t = 0.7MPa$$
  $S_c = 5MPa$   $E = 10GPa$  
$$\nu = 0.3 \qquad \varphi = 20^{\circ}$$
 (58)

typical for ice, cf. Sunder and Connor (1984). The problem parameters are D, h, n, \alpha\_t and C\_1. The experimental data indicate that for brittle materials the critical stress for punch indentation is of the order of  $p_c/S_c = 4-10$ , cf. Wijk (1989), and the cracked zone radius reaches the values  $r_e/D = 2-8$ , cf. Pang et al (1990). For the plane strain case, the cracked zone and punch pressure evolution are shown in Fig. 7-8 as functions of punch displacements  $u_f/D$  for different values of the angle  $\alpha_I$  of cracked zone (assumed  $\kappa = 0$ ). It is seen that the predicted values are within the range of experimental observation. For specified values of  $\alpha_I$ , the growth of cracked zone and maximal pressure is due to growth of the length of shear band in the final failure mode. Figures 9-10 show the respective curves for the plane stress case. The experiments carried for ice plates indicate that the maximal stress is reached at small punch displacements with subsequent drastic reduction of pressure for progressive punch penetration, cf. Michel and Toussaint (1977). The same character of load-displacement diagram was predicted by the present model. The effect of crack number on variation of buckling mode from in-plane to out-of-plane is illustrated in Fig. 11. Here the plot of lines  $k_t = k_z$  are shown with in-plane buckling (W) occurring below the curve and out-of-plane buckling occurring above the curve (Z). The effect of buckling

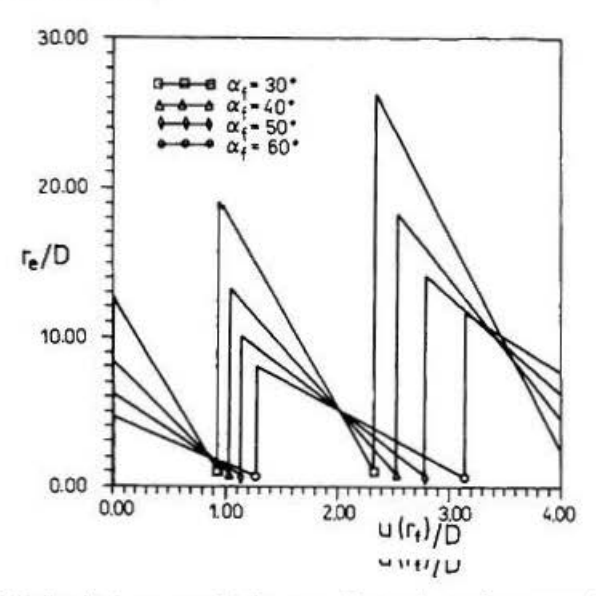


Figure 7: Relation between cracked zone radius and punch penetration depth (plane strain case)

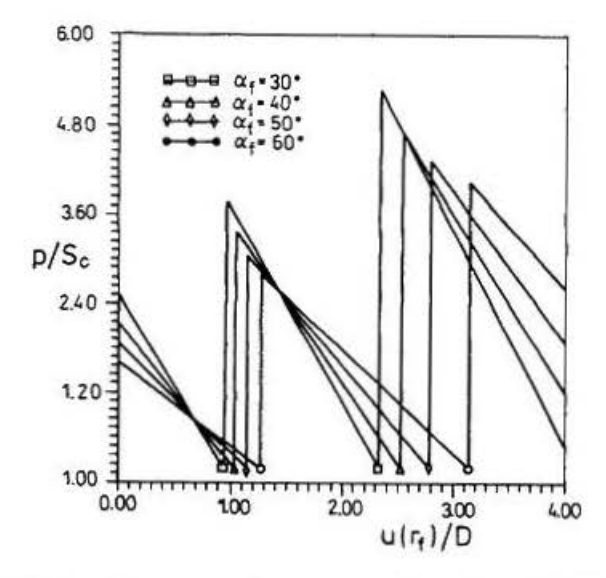


Figure 8: Relation between punch pressure and punch penetration depth (plane strain case)

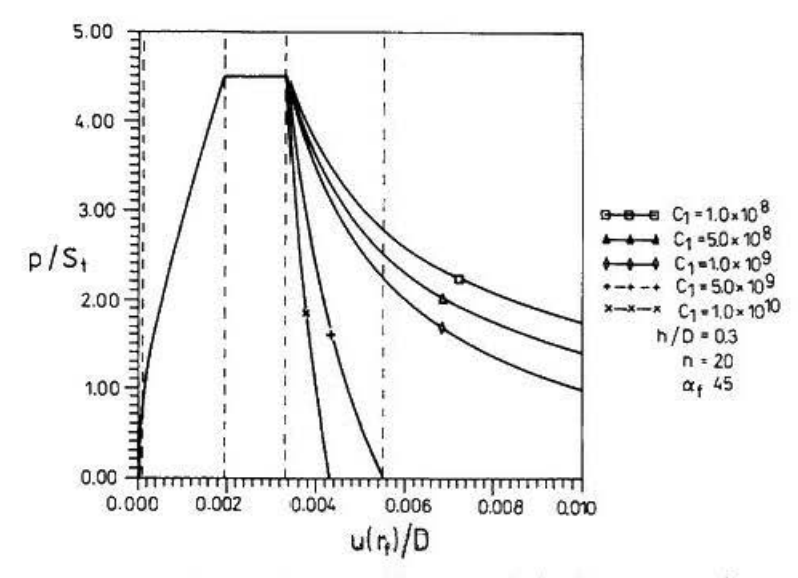


Figure 9: Influence of hinge softening stiffness on relation between punch pressure and punch penetration depth (plane stress case)

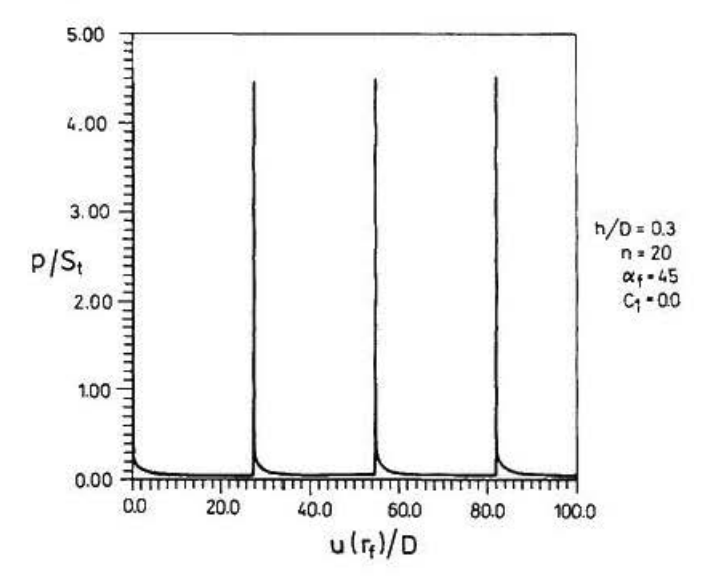


Figure 10: Relation between punch pressure and punch penetration depth (plane stress case)

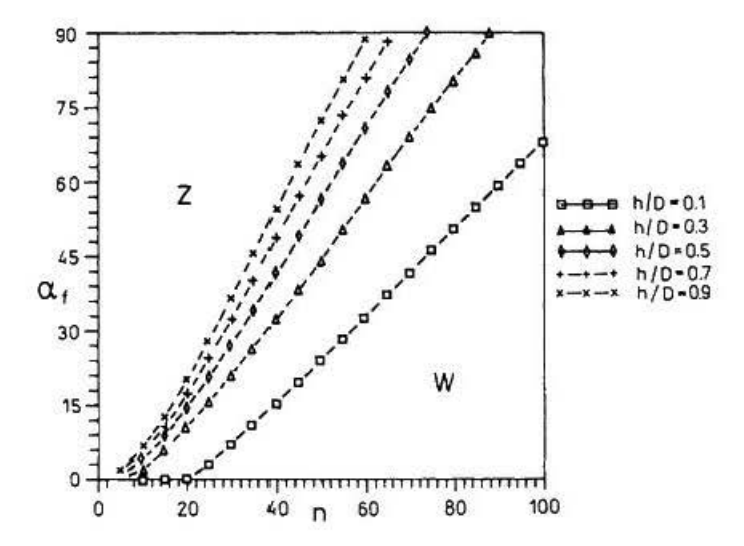


Figure 11: Effect of crack number on variation of buckling mode

mode leads to a new idea of damage mechanism in brittle materials. The buckling of cracked material was also considered by Bažant et al (1993).

#### 5 Concluding Remarks

The present analysis provides the insight into the progression of failure modes in brittle materials. These are termed as cracking, crushing, buckling, post-buckling and shearing modes. The analysis of consecutive modes and of their interaction provides the resulting force-displacement diagram, usually of oscillating character, indicating periodicity of mode evolution. The qualitative assessment provides results confirmed by experimental data and observation. A more refined analysis is needed predicting number of cracks and their evolution. However such analysis would be much more complex.

#### References

Bažant, Z. P., Lin F. B. and Lippmann, H. (1993) Fracture Energy Release and Size Effect in Borehole Breakout. Int. J. Numerical & Analytical Methods in Geomechanics, 17.

Bažant, Z. P. and Ohtsubo, H. (1977) Stability conditions for propagation of a system of cracks in a brittle solid. Mech. Res. Comm. 4, 353-366.

- Cook, N. G. W., Hood, M. and Tsai, F. (1984) Observations of Crack Growth in Hard Rock Loaded by an Indenter. Int. J. Rock Mech. Min. Sci. & Geomech. Abstr., 21, 97-107.
- Dems, K. and Mróz, Z. (1985) Stability Conditions for Brittle-Plastic Structures with Propagating Damage Surfaces. J. Struct. Mech., 13, 95-122.
- Derski, W., Izbicki, R., Kisiel, I. and Mróz, Z. (1989) Rock and Soil Mechanics, Elsevier.
- Ewy, R. T. and Cook, N. G. (1990) Cylindrical Opening in Rock. Int. J. Rock Mech. Min. Sci. & Geomech. Abstr., 27.
- Hellan, K. (1984) An Asymptotic Study of Slow Radial Cracking. Int. J. Fracture, 26, 17-30.
- Jaeger, J. C. and Cook, N. G. W. (1976) Fundamentals of Rock Mechanics., John Wiley & Sons, New York.
- Kowalczyk, M. and Mróz, Z. (1988) Analysis of the cracking and crushing mechanism around the opening in brittle materials. (in Polish). Archives of Mining Sciences, 33, 403-439.
- Klisiński, M. and Mróz, Z. (1988) Stability conditions for brittle-plastic structures with propagating damage surfaces. Int. J. Solids Struct., 24, 391-416.
- Ladanyi, B. (1967) Expansion of Cavities in Brittle Media. Int. J. Rock Mech. Min. Sci., 4, 301-328.
- Lindqvist, P. and Lai Hai-Hui, (1983) Behaviour of the Crushed Zone in Rock Indentation. Rock Mech. Rock Engng., 16, 199-207.
- Michel, B. and Toussaint, N. (1977) Mechanisms and Theory of Indentation of Ice Plates. J. Glaciology, 19, 285-300.
- Mróz, Z. and Drescher, A. (1968) Limit Plasticity Approach to Some Cases of Flow of Bulk Solids. Transactions of the ASME, 1-8.
- Pang, S. S., Goldsmith, W. and Hood, M. (1989) A Force-Indentation Model for Brittle Rocks. Rock Mech. and Rock Engng., 22, 127-148.
- Pang, S. S. and Goldsmith, W. (1990) Investigation of Crack Formation During Loading of Brittle Rock. Rock Mech. and Rock Engng., 23, 53-63.
- Sunder, S. S. and Connor, J. J. (1984) Numerical Modeling of Ice-Structure Interaction. MIT Report.

- Swain, M. V. and Lawn, B. R. (1976) Indentation Fracture in Brittle Rocks and Glasses. Int. J. Rock. Mech. Min. Sci. & Geomech. Abstr., 13, 311-319.
- Tokar, G. (1990) Experimental Analysis of the Elasto-Plastic Zone Surrounding a Borehole in a Specimen of Rock-Like Material Under Multiaxial Pressure. Engng. Fracture Mechanics, 35, 879-887.
- Wagner, H. and Schümann, E. H. R. (1971) The Stamp-Load Bearing Strength of Rock an Experimental and Theoretical Investigation. Rock Mechanics, 3, 185-207.
- Wijk, G. (1989) The Stamp Test for Rock Drillability Classification. Int. J. Rock Mech. Min. Sci. & Geomech. Abstr., 26, 37-44.
- Życzkowski, M. (1956) Calculation of critical forces for elastic tapered beams, (in Polish). Rozpr. Inż., IV, 367-412.